Twenty-Second Symposium (International) on Combustion/The Combustion Institute, 1988/pp. 455–463

PREDICTION OF KNOCK OCCURRENCE IN A SPARK-IGNITION ENGINE

KWANG MIN CHUN, JOHN B. HEYWOOD AND JAMES C. KECK
Sloan Automotive Laboratory
Massachusetts Institute of Technology
Cambridge, Massachusetts 02139

It is generally accepted that knock in a spark-ignition engine is caused by end-gas autoignition. Hu and Keck have recently developed a reduced kinetic model which simulates the kinetic processes involved in autoignition of hydrocarbon-air mixtures. The model was used successfully to correlate measurements of explosion limits in a constant volume bomb and ignition delay times in rapid compression machines. In this paper, the ability of Hu and Keck's model to predict the onset of knock in a spark-ignition engine is evaluated.

Experimental data from a large number of individual cycles were generated from a single-cylinder engine over a range of operating conditions where knock occurred. The unburned gas temperature used in the kinetic model was calculated from the measured cylinder pressure data assuming that knock originates in that part of the end-gas region which is compressed adiabatically.

The model indicates that autoignition under knocking conditions is a two stage process. The model predictions of when knock occurs generally match well with measured knock angle on a cycle-by-cycle basis for a range of fuel (isooctane, primary reference, and indolene) and engine operating conditions. Agreement is least satisfactory when knock occurs close to the end of the burning process when the end-gas mass fraction is small and its temperature is not known precisely.

Introduction

Knock currently prevents increasing the compression ratio of a spark-ignition engine to improve its energy conversion efficiency. Much effort has been devoted to inhibiting knock either mechanically by improving the chamber design or chemically by changing the molecular structure of fuel.[1,2] However, our ability to extend the knock limits of a spark-ignition engine is limited by our lack of fundamental knowledge of the processes which cause knock in the engine and especially of the chemical mechanisms which lead to autoignition.

Chemical kinetic models for autoignition of high pressure and temperature fuel-air mixtures fall into three categories: simple empirical relations (often of the Arrhenius form), models which include all the elementary reactions which might occur, and models where only the rate-limiting reactions are included. Empirical relations[3,4,5] are too simple to give any information about the reaction process and at best only fit the data over a limited range. The complete models often include several hundred reactions even for simple fuels. The most comprehensive model which has been tested is the mechanism developed by Westbrook, Dryer, Pitz, and co-workers.[6,7,8] The fuels modeled to date are methane, n-butane and isobutane. Dimpelfeld and Foster[9] tested the model and found that the initial temperature at the time of spark must be increased above the bulk temperature for the predicted time of autoignition to agree with the observed time. Leppard[10] showed that this model's predictions agreed to within two crank angle degrees of experimental data for ethane-air mixtures. Westbrook and co-workers model has been developed so far for lower hydrocarbons which have different ignition characteristics compared to higher hydrocarbons.[11]

Researchers at Shell's Thorton Research Center[12,13,14] developed a generalized chemical model based on the degenerate branched-chain mechanism of Semenov.[15] This autoignition model has been tested in the spark-ignition engine combustion simulations by Natarajan and Bracco,[16] Schapertons and Lee,[17] and by Najt.[18] Although the results show the usefulness of this model, it must be calibrated for each fuel used and there is no direct correspondence between the model parameters and elementary reaction rate-constants. Cox and Cole[21] refined and expanded the Shell model but some of the reaction constants they needed to fit autoignition data vary by orders of magnitude from currently available fundamental kinetic data.

Benson[22] has reviewed the chemical kinetic

mechanisms involved in hydrocarbon oxidation and summarized the relevant reaction rate-constants. Recently, Hu and Keck[19,20] developed a model based on Benson's work with a mechanism similar to Cox and Cole's. The model predictions have been compared with explosion limits in a constant volume bomb measured at M.I.T.,[19,20] and with ignition delay times in rapid compression machines measured at M.I.T.[23] and Shell's Thornton Research Center.[13] Good agreement between measured and calculated values was obtained with only minor adjustments in published rate constants.

In a spark-ignition engine the unburned mixture (or end-gas) environment is more complex than that of an RCM or bomb. There is turbulence, nonuniform gas composition due to incomplete fuel air residual-gas mixing, a cold boundary layer adjacent to the combustion chamber wall, and changing gas pressure and temperature. Also, the time scale of the varying gas state depends on the engine's speed. In this paper, the model developed by Hu and Keck was tested for its ability to predict the onset of knock in a spark-ignition engine. Experimental data was generated under knocking conditions at wide-open throttle for several fuels and a range of engine speeds. Cylinder pressure records from many individual cycles were used to estimate the temperature in the adiabatic core of the end-gas in each of these cycles as a function of time. The measured pressures and initial temperatures for each cycle were the inputs to the model; the predicted time of knock occurrence and the measured time of occurrence were then compared.

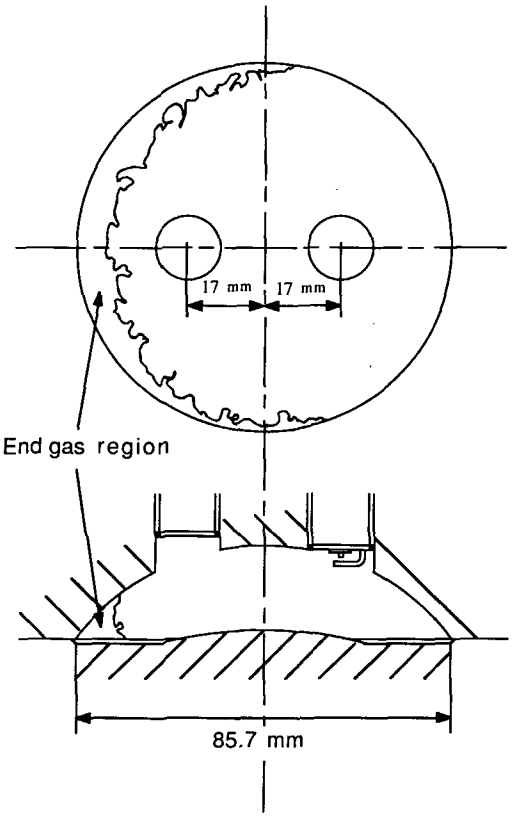

FIG. 1. Engine geometry showing spark plug and pressure transducer positions and location of end-gas region for the Ricardo single cylinder spark-ignition engine.

Experimental Apparatus

A Ricardo Hydra III single-cylinder spark-ignition engine was used for the experiments. The engine, as shown in Fig. 1, has a hemispherical combustion chamber with a compression ratio of 8.29. The bore was 85.7 mm and stroke 86.0 mm. The cylinder pressure was measured by a Kistler 7061 water-cooled transducer mounted at the opposite side of the cylinder axis to the spark plug. The pressure data was digitized, and the data sampling rate was increased during the combustion process to obtain accurate pressure records prior to and after onset of knock. During this period, data was sampled at every 1/11th crank angle degree. Isooctane, of reaserch octane number (RON) 100, indolene (RON of 97.4) and a primary reference fuel (PRF: mixtures of isooctane and n-heptane) of RON 94 were used as fuels. Indolene was injected into the intake port with a conventional electronic fuel-injection system. Isooctane and the primary reference fuel were premixed in a large heated tank upstream of the intake port to ensure mixture uniformity. Experimental conditions for different data sets are reported in Table I.

Chemical Kinetic Model

The nineteen generic reactions included in the kinetic model are listed in Table II along with Arrhenius parameters for the equilibrium and rate constants. The values of the parameters are based on available experimental data and estimates made by Benson[22] using transition state theory and group additivity. The forward and reverse rate constants k^+ and k^- are related to the equilibrium constant K based on concentration by the detailed balancing condition $k^+ = k^-K$.

An essential feature of the model is its ability to reproduce the well known two-stage ignition characteristic of larger hydrocarbons in the high pressure and low temperature region. This characteristic is a consequence of reactions 2-10 in the model.

Table I
Experimental Conditions[a]

Data Set	Speed (rev/min)	Inlet temp (C)	Spark timing[b]	Equiv. ratio	Fuel type	RON	$\bar{\theta}_k$[d]
1	1500	88	40	1.06	Isooctane	100.	1.8
2	1500	22	40	1.04	PRF[c]	94.	4.4
3	1500	21	25	1.00	PRF[c]	94.	19.9
4	2500	31	38	1.01	Indolene	97.4	13.8
5	1500	23	40	1.00	Indolene	97.4	4.7
6	1000	33	20	1.01	Indolene	97.4	17.4

[a]All experiments at wide open throttle.
[b]Crankangle degrees before top center.
[c]Primary reference fuel (mixture of isooctane and n-heptane).
[d]$\bar{\theta}_k$ is the mean value of the knock occurrence crank angle in degrees after top center.

During the first stage, reactions 2-7 form a degenerate branched chain which causes exponential growth in the concentrations of active radicals and the low temperature branching agent ROOH. In this stage, the chemical energy released is negligible. Branching ceases and the second stage begins when the temperature rise due either to compression or chemical energy release reaches the point where the removal of active radicals by the terminating reaction 8 exceeds the production in reaction 7. During this stage, the concentration of ROOH decreases to a quasi-steady value but the

Table II
Chemical Kinetic Model (Units: cc, mole, sec, kcal)

Arrhenius parameters for the equilibrium constant $K = A\ e^{-E/RT}$ and rate constants $k^{\pm} = A^{\pm}\ e^{-E^{\pm}/RT}$ for isooctane oxidation at $700 < T < 1300$ K

Reaction	$\Delta H_{300°}$	log A	E	log A^+	E^+	log A^-	E^+
1 RH + O_2 ↔ $\dot{R}$ + $H\dot{O}_2$	46.4	1.5	46.0	13.5	46.0	12.0	0
2 $\dot{R}$ + O_2 ↔ $R\dot{O}_2$	−31.0	−1.4	−27.4	12.0	0.0	13.4	27.4
3 $R\dot{O}_2$ ↔ $\dot{R}$OOH	7.5	0.0	11.4	11.0	21.4	11.0	11.0
4 $\dot{R}$OOH + O_2 ↔ $\dot{O}_2RO_2H$	−31.0	−1.9	−27.4	11.5	0.0	13.4	27.4
5 $\dot{O}_2RO_2H$ → OROOH + OH	−26.6			11.3	17.0		
6 $\dot{O}$H + RH → $\dot{R}$ + H_2O	−23.5			13.3	3.0		
7 OROOH → $\dot{O}$H + OR$\dot{O}$	43.6			15.6	43.0		
8 $\dot{R}$ + O_2 ↔ $H\dot{O}_2$ + C = C	−13.5	0.0	−13.5	11.5	6.0	11.5	19.5
9 $H\dot{O}_2$ + $H\dot{O}_2$ → HOOH + O_2	−38.5			12.3	0.0		
10 HOOH + M → 2$\dot{O}$H + M	51.4			17.1	46.0		
11 OR$\dot{O}$ → R′CHO + $\dot{R}$″O	8.5			14.0	15.0		
12 $\dot{R}$″O + O_2 ↔ $\dot{O}_2$R″O	−31.0	−1.9	−27.4	11.5	0.0	13.4	27.4
13 $\dot{R}$OOH → $\dot{O}$H + R′CHO + C = C	−3.0			14.4	31.0		
14. $R\dot{O}_2$ + R′CHO → ROOH + $\dot{R}$′CO	−0.6			11.45	8.6		
15 $R\dot{O}_2$ + RH ↔ $\dot{R}$ + ROOH	8.0	1.1	8.0	11.2	16.0	10.1	8.0
16 $H\dot{O}_2$ + R′CHO → HOOH + $\dot{R}$′CO	−0.6			11.7	8.6		
17 $H\dot{O}_2$ + RH ↔ $\dot{R}$ + HOOH	8.0	0.9	8.0	11.7	16.0	10.8	8.0
18 $H\dot{O}_2$ + C = C → Epox + $\dot{O}$H	−0.23			10.95	10.0		
19 $\dot{R}$ + $\dot{R}$ → RH	−85.0			13.2	0.0		

NOTE: ROOH is grouped with OROOH and $\dot{R}$′CO is grouped with $\dot{R}$″O.

temperature and concentration of the high temperature branching agent HOOH continue to rise. The second stage ends in a branched thermal explosion when the rate of the HOOH decomposition via reaction 10 exceeds that of the terminating reaction 8 and branching resumes. It is this explosion which causes the audible knock in spark-ignition engines.

A second essential feature of the kinetic model is its ability to explain the dependence of the explosion limits on fuel structure. The reaction which depends most strongly on fuel structure is the isomerization reaction 3. In the pressure and temperature range of interest this reaction is in equilibrium and it is therefore the equilibrium constant K_3 which is important. In addition, recent measurements by Slagel et al.,[24] brought to our attention by one of the referees, indicate that the equilibrium constant for reaction 2 depends to some extent on fuel structure. More importantly, these measurements suggest that the reaction enthalpy for attachment of an 0_2 molecule to a secondary hydrogen site should be -37 kcal rather than the -31 kcal estimated by Benson from group additivity. Although this work is of considerable significance for the thermodynamics and kinetics of hydrocarbon combustion, in the present model it is the product K_2K_3 which is important and this product is only slightly altered by the new results. Moreover since the value of K_3 for isooctane was obtained by fitting data from constant volume bomb and rapid compression machines, any change in the value of K_2 will result in a corresponding change in the value of K_3 which leaves the product K_2K_3 invariant. For the other fuels studied in the present work values of K_3 were not available and the activation energy E_3 for each fuel was adjusted to give the best fit with the measurements.

It should be noted in connection with the above discussion of reaction 3 that the isomerization rates of $\dot{O}_2R''O$ and $\dot{O}_2R'CHO$ have been assumed negligible compared to that for $R\dot{O}_2$ because of the smaller number of carbon atoms in these radicals. It may also be noted that reactions 13-19 as well as a number of other radical-radical and radical-intermediate reactions not included in the model were found to be of secondary importance compared to reactions 1-12. In general omission of these reactions produces changes which are small compared to those due to uncertainties in the rate constants used.

End-Gas Temperature Calculation

Due to the temperature sensitivity of the reactions involved, it is expected that knock will occur first in the adiabatic core of the unburned end-gas ahead of the flame. To calculate the temperature of this core gas, it is assumed that: 1) The thin reaction sheet separating burned and unburned gas in the cylinder is of negligible thickness; 2) The boundary layers are sufficiently thin so that adiabatic cores exist in both burned and unburned gases; 3) The rates of compression, burning and end-gas reaction prior to knock are sufficiently slow so that the pressure throughout the cylinder is uniform; 4) The burned and unburned gases may be approximated as ideal gases having locally constant specific heats.

It is further assumed that knock occurs when the rate of reaction in the end-gas becomes so large that assumption 3 is no longer valid and observable pressure fluctuations occur due to the propagation of shock and sound waves in the gas. Knock will, of course, be delayed or suppressed when the smallest dimensions of the end-gas region, shown schematically in Fig. 1, become comparable to that of the boundary layers and assumption 2 fails.

With these assumptions, the energy equation for the unburned core gas may be written

$$\left(\frac{\gamma_u}{\gamma_u - 1}\right)\frac{\dot{T}_u}{T_u} = \frac{\dot{p}}{p} + \frac{\dot{q}_u}{R_u T_u} \tag{1}$$

where

$$\dot{q}_u = -v_u \Sigma \Delta H_i (r_i^+ - r_i^-). \tag{2}$$

is the specific chemical energy release rate due to end-gas reactions, T is the temperature, p is the pressure, v is the specific volume, γ is the specific heat ratio c_p/c_v, R is the universal gas constant, ΔH_i is the molar enthalpy change for reaction i, r_i^+ and r_i^- are the forward and reverse reaction rates per unit volume for reaction i, and the subscript u refers to the unburned core gas.

Given models for the burning rate and boundary layer growth, and using the value of $\dot{q}_u$ provided by the kinetic model, $\dot{p}/p$ could be predicted and Eq. (1) used to obtain the end-gas core temperature as a function of time. However, it can be shown using the ideal gas law and energy conservation for the unburned and burned gas cores that neglecting the effect of $\dot{q}_u$ on p results in an error in T_u given approximately by

$$\frac{\Delta T_u}{T_u} \approx \left(\frac{\gamma_{u-1}}{\gamma_u}\right)\frac{x_u}{(1 - x_u)}\frac{q_{us}}{c_{vb}T_b} \tag{3}$$

where x_u is the unburned core-gas mass-fraction of the and q_{us} is the specific chemical energy released from the time of spark discharge in the unburned core. In the present experiments the maximum value of x_u at knock was $\sim$0.2 and the maximum value of q_{us}/c_{vb} was $\sim$300 K. Assuming $\gamma_u \sim 1.3$ and $T_b \sim 3000$ K we find from Eq. (3) that $\Delta T_u/T_u \sim 0.005$. This error is significantly less than the errors as-

sociated with the determination of the initial temperature of the gas at spark and the modeling of the burning rate, boundary layers, and leakage in spark-ignition engines. We have therefore chosen to integrate Eq. (1) using the measured pressure-time curves as input rather than attempting to use a predictive model.

The calculations were started at 90 °BTC where the mean gas temperature was computed from the equation of state $\bar{T}_i = p_i V_i/(mR_u)$ using measured values for p_i, V_i and m. At this point $\bar{T}_i$ was approximately equal to the wall temperature so that the assumption of uniform initial temperature should be reasonably good. Prior to knock the pressure data were smoothed to eliminate high frequency fluctuations and improve accuracy. Eq. (1) was integrated in conjunction with 14 kinetic rate equations using the GEAR method.[25] Knock was assumed to occur when

$$\dot{T}_u/T_u \approx \dot{v}_u/v_u > \varepsilon/\tau_a \qquad (4)$$

where $\tau_a \sim 0.1$ ms is the transit time of a sound wave across the cylinder and ε is an arbitrary fraction. Due to the rapid rate of increase in v_u just prior to knock, the determination of the knock point is insensitive to the exact choice of ε and changing its value from 0.1 to 1.0 resulted in a change of less than one degree in the predicted knock onset crank angle. In the present work ε was set equal to one.

To extend the calculations beyond the observed knock point in cases where the model failed to predict knock, smooth second order extrapolations of the pressure curves prior to knock were used. In none of the cases reported was it necessary to extend the curves more than 5 CA°.

Results and Discussion

It is well known that the combustion process in a spark-ignition engine varies substantially from cycle-to-cycle. As a consequence, knock occurrence varies cycle-by-cycle, largely due to variations in end-gas state which these burning rate variations produce. Figure 2 shows a typical distribution in knock occurrence crank angle for 398 consecutive cycles at fixed engine operating conditions. The time of knock occurrence was defined as the point where the time scale for pressure $p/\dot{p}$ was shorter than 0.2 ms. Pressure traces for six cycles of one isooctane fueled experiment are shown in Fig. 3. These cycles were chosen for their different combustion rate history. Generally knock occurs earlier for faster burning cycles. Clearly prediction of knock onset with kinetic models should be done on an individual cycle basis.

The model predictions of crank angle of knock occurrence for isooctane are compared with measured values in Fig. 4. The value used for the activation energy E_3 in the equilibrium constant for reaction 3 was 11.4 kcal/mole, which is the same as the value used by Hu and Keck for isooctane. The predictions match the measurements to within about 3 crank angle degrees without any adjustment in the reactions or the reaction constants. E_3 was changed to 11.2 kcal/mole to test the sensitivity of the model to the value of this activation energy; the predicted knock occurrence angle was decreased by 0.2 crank angle degree. The initial mass inside the cylinder is required to estimate the initial mixture temperature. The accuracy of the estimate of initial mass (fresh fuel and air plus residual gas) is about 2 percent for this experiment. The

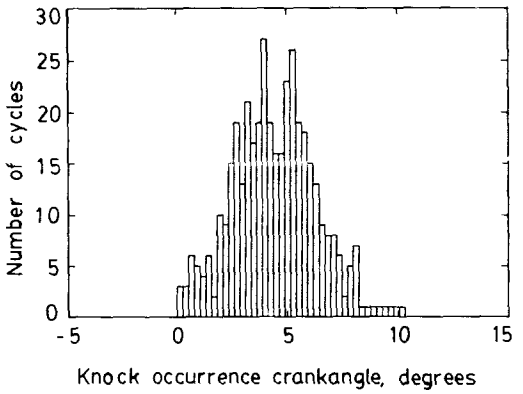

FIG. 2. Individual-cycle knock occurrence crank angle distribution for 94 RON primary reference fuel at 1500 rev/min, spark timing at 40 degrees before TC and wide-open throttle. 0 degrees = top center. Data set 2.

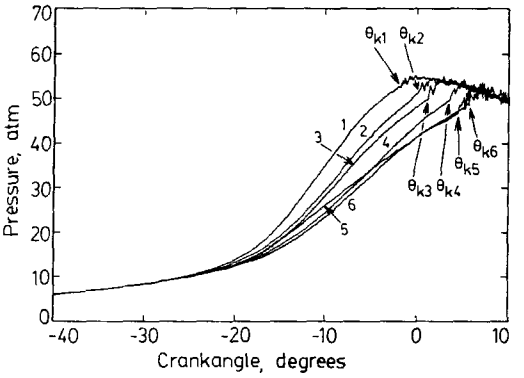

FIG. 3. Pressure traces for six individual cycles, isooctane fuel, spark timing at 40 degrees before TC, engine speed 1500 rev/min, wide open throttle, fuel/air equivalence ratio = 1.06. 0 degrees = top center. Data set 1.

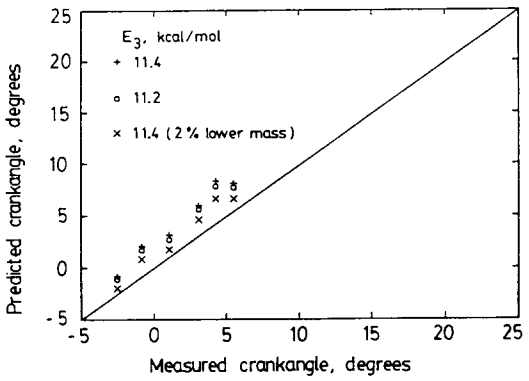

FIG. 4. Comparison of measured and predicted knock occurrence crank angles for isooctane-fueled experiment. 0 degrees = top center. Same conditions as in Fig. 3.

initial mass was lowered 2 percent to assess the impact of this uncertainty; this change results in about 1.5 crank angle degrees earlier prediction of knock onset.

Results with a primary reference fuel of RON 94 (94 percent isooctane and 6 percent n-heptane) at 1500 rev/min and those with indolene of RON 97.4 at 1000, 1500, and 2500 rev/min are shown in Fig. 5. Indolene is a blended gasoline used for engine testing and consists of a large number of saturated, olefin and aromatic hydrocarbon compounds. The engine speed was 1500 rev/min and the spark timings were 40 and 25 degrees before top center (BTC)

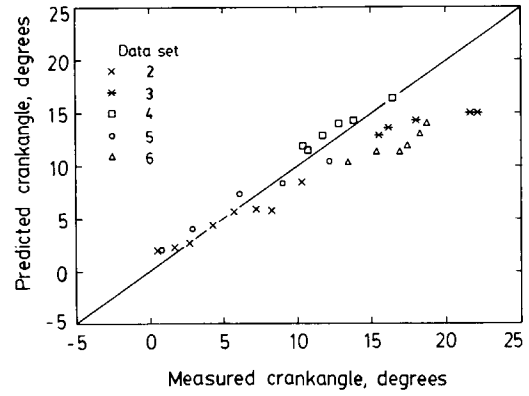

FIG. 5. Comparison of measured and predicted knock occurrence crank angles (after top center, 0 degrees): for primary reference fuel with 94 RON, wide-open throttle, 1500 rev/min (data sets 2 and 3); and for indolene fuel at wide open throttle, engine speeds of 2500, 1500, and 1000 rev/min, and spark timing 38,40,20 degrees before TC, respectively (data sets 4, 5, and 6).

for 94 RON PRF. Since we have no fundamental data for blended fuels for the activation energy E_3, it was adjusted by trial and error for the different fuels used. E_3 was used because it is the least well known and most sensitive fuel dependent parameter. Values of E_3 were chosen which gave the best comparison between the measured and calculated knock occurrence crank angle for the cycles of one data set: the 40 BTC timing case was used for the 94 RON PRF and the 1500 rpm case was used for indolene. The best fits were obtained with activation energies E_3 of 11.2 kcal/mole for indolene and 11.0 kcal/mole for 94 RON PRF. These values are between that for isooctane (11.4) and for *n*-heptane (8.0) measured by Hu and Keck.[20]

The one parameter fit calculations match well with measurements for the primary reference fuel where knock occurs before about 15 °ATC, and at engine speeds of 2500 and 1500 rev/min for the indolene fuel. Agreement is less good for slower-burning cycles where knock occurred late in the combustion process for 94 RON PRF cases and at 1000 rev/min for indolene. The model predicts knock occurrence too early for later and slower burning cycles, and at low engine speed.

Sample end-gas temperature profiles are shown in Fig. 6. The dotted line shows the temperature calculated from Eq. (1) without reaction energy release in the end-gas. This energy release which is associated with the second stage starts well before knock occurrence. The end-gas energy release with 94 RON PRF is more significant than with isooctane fuel, and the concentration of ROOH was higher at the end of the first stage of ignition than the isooctane case. Also, the slower combustion cycles shows a higher energy release rate than that of the faster combustion cycle. This reduces the du-

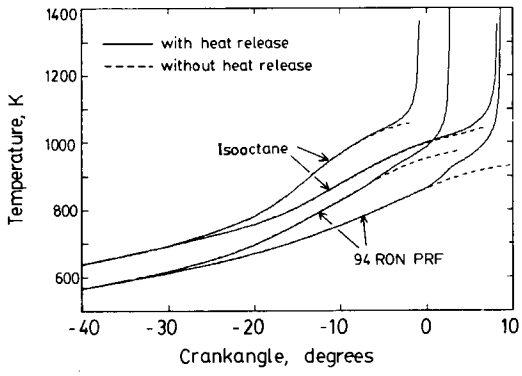

FIG. 6. Predicted end-gas temperature profiles for cycles 1 and 6 for isooctane-fueled experiment in Fig. 3, and for a faster and slower burning cycle with 94 RON primary reference fuel at 1500 rev/min and wide-open throttle (data set 2). 0 degrees = top center.

ration of the second stage ignition process for these slower combustion cycles.

Summary and Conclusions

In summary, the Hu and Keck kinetic model for autoignition, applied on an individual cycle basis, coupled with an adiabatic core assumption for the critical end-gas region predicts knock occurrence which agrees within a few crankangle degrees with experimental data for isooctane, a primary reference fuel, and indolene in a standard spark-ignition engine. Agreement is least satisfactory when knock occurs late in those cycles where the combustion process is slower (e.g., at low engine speeds and in slower-burning cycles at higher speeds) where knock predictions are too early. Late in the combustion process as the flame propagates into the end-gas thermal boundary layer, the end-gas temperature will fall below the adiabatic core temperature used for these predictions. The poorer agreement between predictions and data for late occuring knock, and at lower speeds where the boundary layer has more time to grow to a greater thickness, is most likely due to this reduction in end-gas temperature under these conditions.

The following conclusions may be drawn:

1) For isooctane, the Hu and Keck model can be used to predict knock occurrence crank angles in a spark-ignition engine on a cycle-by-cycle basis within experimental error using previously determined values for the rate constants and assuming that for the range of conditions investigated the end-gas is adiabatically compressed.

2) For 97.4 RON indolene and 94 RON primary reference fuel, a one parameter fit of the model to the data for the faster burning cycles and the higher engine speeds can be obtained by adjusting the activation energy of the equilibrium constant for the isomerization reaction $R\dot{O}_2 \rightarrow \dot{R}OOH$.

3) For slower burning cycles when knock occurs late, well after the top center crank position, and at low engine speed, the measured knock occurrence crank angles are larger than those predicted by the model. This discrepancy is most likely due to a reduction in the end-gas temperature due to mixing of cold gas from the boundary layer and the side wall vortex with the adiabatic core gas.

4) The observations are consistent with a two-stage autoignition process.

5) Considering our assumption that knock occurs first in the adiabatic core of the end-gas and the sensitivity of the model to the reaction rate constants, the agreement between theory and experiment is encouraging. More work is clearly needed to determine the effects of mixing on the end-gas temperature and to improve our knowledge of the critical reaction parameters especially for blended fuels.

Acknowledgment

This work has been sponsored by the M.I.T. Sloan Automotive Laboratory's Consortium for Engine Research. Member companies supporting this effort were: Ford Motor Company, Peugeot Societe Anonyme, and Regie Nationale des Usines Renault. It was also supported by the U.S. Department of Energy, Office of Energy Utilization Research, Energy Conversion and Utilization Technologies Program.

REFERENCES

1. TAYLOR, C. F.: The Internal-Combustion Engine in Theory and Practice, Vol. II, p. 71, The M.I.T. Press, 1968.
2. OBERT, E. F.: Internal Combustion Engines and Air Pollution, p. 243, Harper & Row, Publishers, 1973.
3. LIVENGOOD, J. C. AND WU, P. C.: Fifth Symposium (International) on Combustion, p. 347, The Combustion Institute, 1955.
4. DOUAD, A. M. AND EYZAT, P.: Four-Octane-Number Method for Predicting the Anti-Knock Behavior of Fuels and Engines, SAE paper 780080 (1978).
5. BY, A., KEMPINSKI, B. AND RIFE, J. M.: Knock in Spark Ignition Engines, SAE paper 810147 (1981).
6. WESTBROOK, C. K. AND PITZ, W. J.: Comb. Sci. Tech. 37, 117 (1984).
7. PITZ, W. J. AND WESTBROOK, C. K.: Comb. Flame 63, 113 (1986).
8. GREEN, R. M., PARKER, C. D., PITZ, W. J. AND WESTBROOK, C. K.: The Autoignition of Isobutane in a Knocking Spark Ignition Engine, SAE paper 870169 (1987).
9. DIMPELFELD, P. M. AND FOSTER, D. E.: Predictions of Autoignition in a Spark-Ignition Engine Using Chemical Kinetics, SAE paper 860322 (1986).
10. LEPPARD, W. R.: Comb. Sci. Tech. 43, 1 (1985).
11. POLLARD, R. T.: Comprehensive Chemical Kinetics (C. H. Bamford and C. F. H. Tipper, Ed.), Vol. 17, p. 249, Elsevier, 1977.
12. HALSTEAD, M. P., KIRSCH, L. J., PROTHERO, A. AND QUINN, C. P.: Proc. R. Soc. Lond. A. 346, 515 (1975).
13. HALSTEAD, M. P., KIRSCH, L. J. AND QUINN, C. P.: Comb. Flame 30, 45 (1977).
14. HIRST, S. L. AND KIRSCH, L. J.: Combustion Modeling in Reciprocating Engines, ed. Mattavi, J. M., and Amann, C. A., p. 193, Plenum Press, New York (1980).
15. SEMENOV, N. N.: Chemical Kinetics and Chain Reactions, Oxford University Press, England (1935).

16. NATARAJAN, B. AND BRACCO, F. V.: Comb. Flame, 57, 179 (1984).
17. SCHAPERTONS, H. AND LEE, W.: Multidimensional Modeling of Knocking Combustion in SI Engines, SAE paper 850502 (1985).
18. NAJT, P. M.: Evaluating Threshold Knock with a Semi-Empirical Model: Initial Results, SAE paper 872149 (1987).
19. KECK, J. AND HU, H.: Twenty First Symposium (International) on Combustion, p. 521, The Combustion Institute, 1988.
20. HU, H. AND KECK, J.: Autoignition of Adiabatically Compressed Combustible Gas Mixture, SAE paper 872110 (1987).
21. COX, R. A. AND COLE, J. A.: Comb. Flame 60, 169 (1985).
22. BENSON, S. W.: Prog. Energy Comb. Sci. 7, 169 (1981) and Oxid. Comm. 2, 169 (1982).
23. TAYLOR, C. F., TAYLOR, E. S., LIVENGOOD, J. C., RUSSEL, W. A. AND LEARY, W. A., SAE Transactions *4* 232 (1950).
24. SLAGEL, I. R., RATAJEZAK, E. AND BUTMAN, D.: J. Phys. Chem. *90* 402 (1986).
25. HINDMARSH, A. C.: GEAR: Ordinary Differential Equation System Solver, UCID-30001, Rev. 3, Lawrence Livermore Laboratory, 1974.

COMMENTS

A. K. Oppenheim, Univ. of California, USA. Following an overwhelming amount of preceding investigations, you identified the onset of knock with what is known as the Frank-Kamenetsky thermal explosion—the rapid rise of temperature following a more-or-less isothermal induction process. As many others, you demonstrated then a most satisfactory agreement between the induction period evaluated on the basis of an adiabatic relation between temperature and pressure measured in an engine with the instant of the detected knock signal. Such coincidence is, of course, a necessary, but by no means a sufficient condition. Knock is, afterall, an explosive phenomenon in more than the Frank-Kamenetsky sense, its onset being associated with the generation of a blast wave similarly as in the case of transition to detonation. Studies of the latter[1] revealed that it depends not only on the induction period you considered, but also on the excitation times as well as the maximum exothermic power,[2] and, in particular, on the rate at which the induction time decreases with temperature. Are you planning to take these effects under consideration in future studies?

REFERENCES

1. A. K. OPPENHEIM, Phil. Trans. Roy. Soc. Lond., Vol. A. 315, pp. 471–508, 1985.
2. "Dynamic Effects of Autoignition Centers of Hydrogen and $C_{1,2}$-Hydrocarbon Fuels" by A. E. LUTZ, et al., This Symposium.

Author's Reply. The influence of detonation waves on knock in S.I. engines is certainly a problem which should be investigated. As pointed out by Oppenheim and his coworkers, such waves would be expected to occur if substantial temperature variations leading to the formation of exothermic centers existed in the unburned end gas. It is anticipated, however, that under most operating conditions the amplitude and length scale associated with such temperature variations will be sufficiently small so that detonation wave, if they occur at all, will be relatively weak.

A. M. Dean, Exxon Research & Engr., USA. Would you compare your E_A = 11.4 kcal/mole for isomerization in isooctane to the recent analysis of Morley on a similar mechanism.

Author's Reply. The value of E_A = 11.4 which we have used in our analysis was obtained from experiments by Hu and Keck[1] in a constant volume bomb and is consistent with hydrogen bond energies given by Kondo and Benson.[2] In the papers by Morley with which we are familiar no value was given for this parameter.

REFERENCES

1. HU, H. AND KECK, J. C., SAE paper 872110, International Fuels and Lubricants Meeting, Toronto, (1987).
2. KONDO, O. AND BENSON, S. W., Intern. J. of Chem. Kinetics, 16, 949 (1984).

●

W. May, Univ. of Kaisaslantern, Fed. Rep. of Germany. Can you include in your model the in-

fluence of Octane Number improving fuel components like methanol, ethanol, MTBE or TAME.

Author's Reply. Our model applies only to alkane fuels with carbon number greater than or equal to 3 for which the rate limiting step is the isomerization reaction $\dot{R}O_2 \leftarrow \dot{R}OOH$. To include the effect of molecules such as methanol, ethanol MTBE or TAME, the oxidation mechanism of these species would have to be known. This is probably the case for methanol and ethanol, however, we are not sure about MTBE and TAME.